ELSEVIER

International Journal of Mass Spectrometry 202 (2000) 55–68

International Journal of Mass Spectrometry

Formation and photophysics of the van der Waals complex ions $[(NO)_x(N_2O_3)_y(FB)_z]^{\pm}$

Xin Yang, Qifei Wu, Yihua Hu, Shihe Yang*

Department of Chemistry, Hong Kong University of Science and Technology, Clear Water Bay, Kowloon, Hong Kong

Received 15 November 1999; accepted 18 February 2000

Abstract

The van der Waals complex ions, $[(NO)_x(N_2O_3)_y(FB)_z]^{\pm}$ (FB = fluoro-benzenes), were produced by supersonic expansion of (NO + FB) seeded in argon and electron impact ionization. Photodissociation and photodetachment of mass-selected complex ions were carried out by time-of-flight mass spectrometry. For the positive cluster ions, $[(NO)_x(N_2O_3)_y(p\text{DFB})_z]^+$, the photofragmentation patterns at $\lambda = 456$ nm and $\lambda = 700$ nm are compared and discussed. At 456 nm, photodissociation of the cluster cations yields extensive fragments, whereas at 700 nm, the photofragments are much suppressed. The fragmentation pattern also exhibits a clear dependence on the cluster size. The photodissociation and photodetachment of the van der Waals complex anions at $\lambda = 456$ nm are compared, showing the competition of two channels, but for $(NO_2\ldots p\text{DFB})^-$, only the photodissociation channel was observed. Photodissociation spectra of mass-selected $NO(FB)^+$ and $(FB)_2^+$ were recorded in the UV-visible spectral region. (Int J Mass Spectrom 202 (2000) 55–68) © 2000 Elsevier Science B.V.

Keywords: van der Waals complex; Photodissociation and photodetachment; Time-of-flight mass spectrometry

1. Introduction

Photodissociation of van der Waals complexes provides important information about intermolecular interaction and molecular dynamics and energetics [1,2]. This study, as a function of system size, raises hopes for bridging the gap in the structure and dynamics between the gas phase and the condensed phase. Van der Waals complexes of benzene and its derivatives attracted extensive interest over the last twenty years [1,3]. For example, during the past few years, the intermolecular rotational and vibrational structures for the complexes between Ar, N_2, and mono-fluoro benzene (FB), mono-chloro benzene (ClB), *o*, *m*, *p*-difluorobenzene (*o*, *m*, *p*-DFB), and xyelene were investigated extensively by this group [4].

The present work is focused on the formation and photophysics of van der Waals complex ions. The primary advantages of studying the photophysics of ions include the relatively easy generation, the ability for mass selection, and the high detection sensitivity. We formed binary van der Waals cluster ions by supersonic expansion of (NO + FB) seeded in argon and electron impact ionization in the jet. Using photodissociation/photodetachment time-of-flight mass spectrometry, branching ratios of the photodissociation and photodetachment channels are studied in terms of their dependence on the wavelengths and

* Corresponding author.

PII S1387-3806(00)00206-2

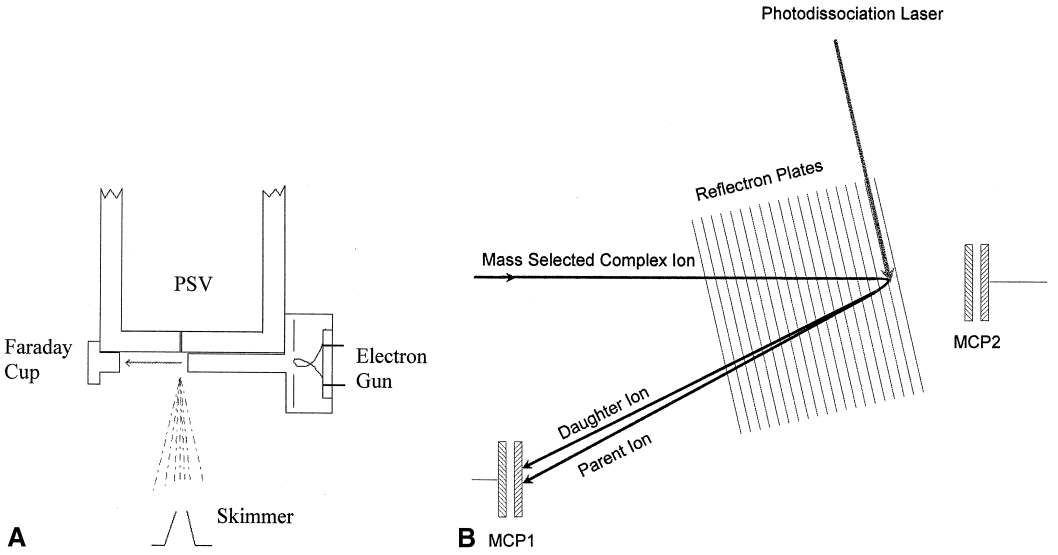

Fig. 1. Schematics of (a) the cluster source and (b) the reflectron region of the time-of-flight mass spectrometer.

cluster size. Photodissociation spectra of mass-selected NO^+. . .FB and $(FB)_2^+$ were recorded in a broad spectral region.

Nitric oxide is known to play an important role in the chemistry of the earth's atmosphere [5]. Recently, it has also been discovered that NO and its positive/negative ions act as "mediators" or "messengers" in a wide range of biological functions [6–8]. Because the energy difference between the ground state and the excited paramagnetic state is around 1/2 kT at room temperature, NO exists as a highly paramagnetic free radical in the gas phase. NO reacts readily with oxygen in the air to form NO_2. NO is thermally unstable and under high pressure breaks down to yield N_2O and NO_2. It is of particular relevance to the present study that nitric oxide ions can form weakly bound complexes with many species such as $NO^+(H_2O)$, $NO^+(CO_2)$, and $NO^+(H_2O \cdot CO_2)$. NO molecules themselves can also bind together to form van der Waals clusters, $(NO)_x$, under supersonic expansion. Their ion intensities were found to show an odd/even alternation [9–11]. These differences in stability were attributed to the spin pairing of valence electrons. Most recently, the van der Waals complexes, $SF_6(NO)_n^+$ and $C_2H_4(NO)_n^+$ have been studied [12–15]. The photodissociation experiments on these weakly bound clusters showed that the intensity of the fragments depends on the cluster size and the wavelengths. The photodissociation channels were investigated under the condition that the ionization potentials (IPs) of the attached species, such as SF_6 and C_2H_4, were higher than those of the nitric oxide clusters, $(NO)_x$.

2. Experimental

The main parts of the experimental apparatus have been described elsewhere [16]. New additions include the electron gun in the cluster source [Fig. 1(a)] and the in-line detection mode for the neutral photofragments [Fig. 1(b)]. The nitric oxide gas (99.5%) was premixed with the FB (including monofluoro-benzene and *p*-difluoro-benzene) vapor at room temperature (~100 Torr) in a reservoir. The mixture was then carried into the pulsed valve by argon (99.5%) with a stagnation pressure of 20 psig. The van der Waals clusters were produced by the supersonic expansion of the mixed gas (FB + NO/Ar) into a high vacuum system from a pulsed valve with an orifice diameter of 0.5 mm (R. M. Jordan Company, Grass Valley, U.S.A.). The neutral vdW clusters were ionized by an electron gun (Daiwa Techno Systems Co. Limited,

Tokyo, Japan) that produced 350 eV electrons and were attached immediately to the exit of the pulsed valve [Fig. 1(a)]. The distance from the orifice of the pulsed valve to the electron beam was 4 mm, and it proved to be critical to the formation of the cluster ions, especially to the formation of negative ions [17]. The cluster ions were extracted vertically 15 cm downstream and accelerated by a two-mode high voltage pulser (~1100 V). The positive mode was for the detection of cations and the negative mode was for the detection of anions.

The extracted cluster ions were steered by a set of vertical and horizontal deflectors, mass selected and reflected by a reflectron block, and finally detected by a dual microchannel plate detector (MCP1). The mass gate was connected to a pulsed high voltage power supply, and the pulse width was variable from 0.5 μs to 1 μs for the selection of a given parent ion. The photodissociation laser was introduced into the vacuum system through a 2.75-in.-diameter quartz window, and aligned vertically in the center of the field-free flight tube just between the last two reflectron plates [see Fig. 1(b)]. The polarity of the reflector and the detector plates could be inverted depending on different requirements for the experiments. An Excimer laser (Lambda Physik LPX210i, 308 nm) pumped a dye laser (Lambda Physik LPD3002), producing a tunable output used as the photodissociation light source. LDS 698, Exalite 398, Stilbene 420, Coumarin 460, Coumarin 540A, Kiton red, DCM, and Coumarin 503 dyes were employed in this study, covering the wavelength range from 400 to 700 nm with a pulse energy of ~10–30 mJ/pulse. Photodissociation of the cluster ions was conducted in the reflectron/detector region [Fig. 1(b)].

The assignment of the fragments was accomplished following the procedure of Duncan et al. [18]. Because photodissociation occurred between the last two reflectron plates, the velocity of the parent ion is approximately zero. After photodissociation, the fragment and the parent ions should have the same kinetic energy, traveling from the point of photodissociation to the detector [MCP1, Fig. 1(b)]

$$(1/2)m_f v_f^2 = (1/2)m_p v_p^2$$

Because $v = L/\Delta t$ (L is the distance from the ion turning point to MCP1), we get,

$$m_f = m_p(\Delta t_f / \Delta t_p)^2$$

In the above equation, m_f represents the mass of the fragment, and m_p represents the mass of the parent ion. v_f and v_p represent the velocities of the fragment and the parent ion. Δt_f and Δt_p are the flight times of the fragment and the parent ion from the point of photodissociation to the detector, respectively.

When a photodetachment experiment on the anions was carried out, the reflectron plate voltages were zeroed, and MCP2 was used instead of MCP1. In order to detect the neutral species after the photodetachment of negative parent ions, MCP2 was applied with a negative high voltage that was normally applied for the detection of positive species. The reason for this setup is as follows. First, the negative high voltage prevented the negative species from arriving at the detector because of the electric repulsion, and therefore mass gate was not needed in this experiment. Second, because the electron-detached clusters or the neutral species were not affected by the electric field before the detector, they traveled at the same velocity as that of their parent anions, and were finally detected by MCP2.

In the reflectron/detector region [Fig. 1(b)], the vacuum was kept on the scale of 10^{-7} Torr. The electric signals from the MCP were further amplified by a Model SR445 preamplifier (Stanford Research) and digitized by a F903 fast transient recorder (USTC, China). The data were transferred to and stored in a PC-486. A typical time-of-flight mass spectrum was obtained based on an average of 100 experimental cycles to enhance the signal to noise ratio. All sequential timing pulses were generated by a Model DG535 delay generator (Stanford Research) that was also controlled by the PC-486.

3. Results and discussion

3.1. Positive van der Waals cluster complexes

3.1.1. The formation of $[(NO)_x(N_2O_3)_y(pDFB)_z]^+$

Shown in Fig. 2 are two time-of-flight mass spectra of the van der Waals cluster cations without and with *p*DFB in the nozzle reservoir, respectively. The clus-

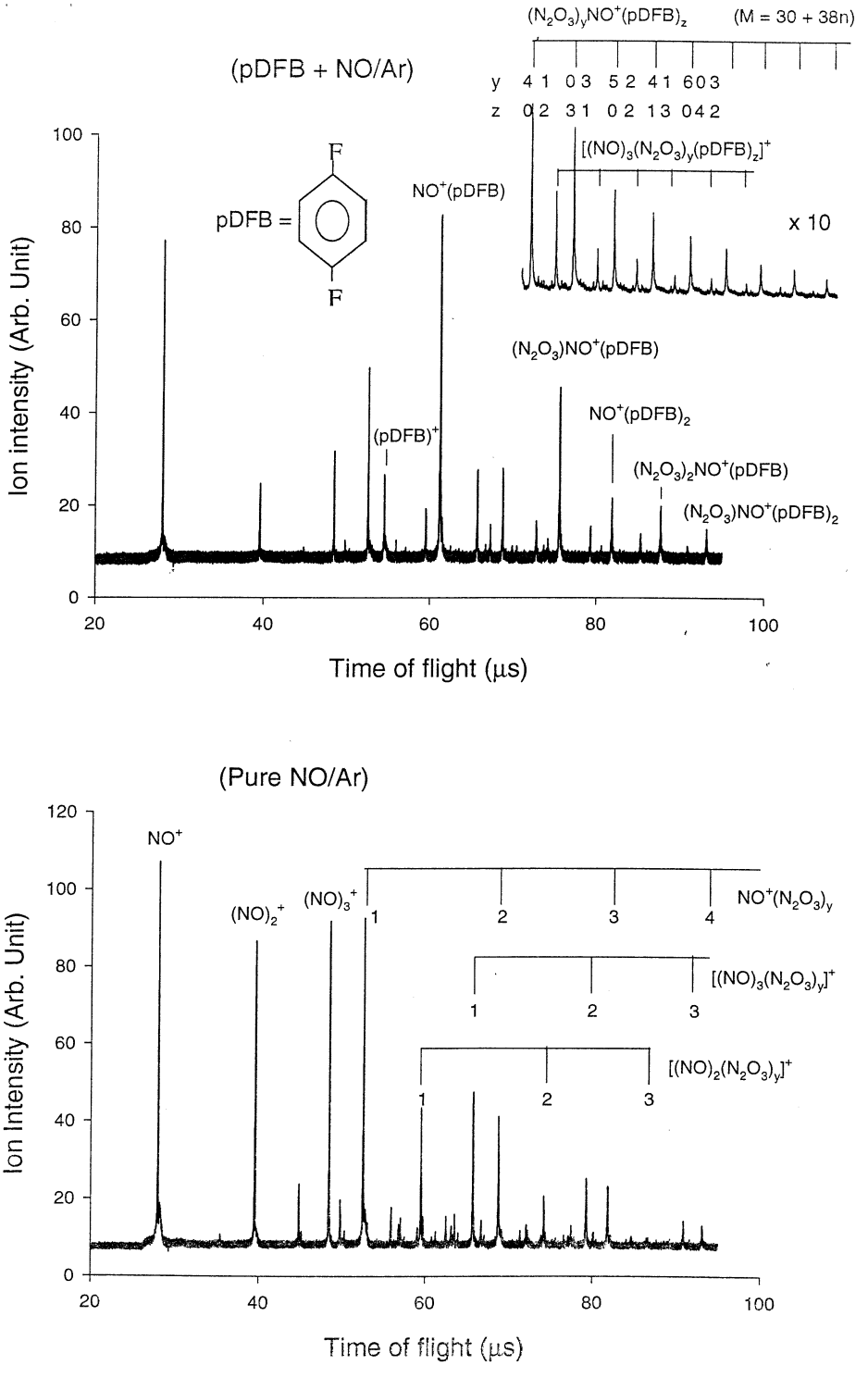

Fig. 2. TOF mass spectra of the van der Waals cluster cations for the system (NO + *p*DFB). Top: with *p*DFB; bottom: without *p*DFB.

ters that were formed when no *p*DFB was added were mainly $(NO)^+_{1-3}$, and three series $NO^+(N_2O_3)_y$, $(NO)^+_3(N_2O_3)_y$, and $(NO)^+_2(N_2O_3)_y$ (Fig. 2, bottom). The peak $(NO)^+_3$ appears to be quite intense; this cluster was observed by Carman et al. and it was suggested to be a stable species [9–11]. In the three cluster series, N_2O_3 seems to be a building block. This species may have been produced from reactions between NO molecules powered by the electron impact. In fact, these cluster species were produced previously by 90 eV electron impact ionization of pure nitric oxide expansions [19] and by secondary ion mass spectrometry (SIMS) on frozen samples of NO [20]. Rydberg charge exchange experiments on nitric oxide expansions yielded negatively charged clusters that also contain building blocks of N_2O_3 [21]. Martin et al. converted nitric oxide clusters completely into $NO^+(N_2O_3)_n$ and $NO^+_2(N_2O_3)_n$ using picosecond UV laser pulses [22]. A chain-type mechanism was proposed for this efficient and selective chemical conversion. We believe that a variant of this mechanism, which embodies a collective intracluster reaction, should be operative in the formation of $(N_2O_3)_n$-containing cluster cations by electron impact ionization.

When *p*DFB is added into the mixture some new peaks appear in the mass spectrum (see Fig. 2, top). Some of the clusters apparently contain *p*DFB molecules. The observed mass peaks for the case of (*p*DFB + NO/Ar) can be represented by $[(NO)_x(N_2O_3)_y(pDFB)_z]^+$ (x = 1–3). For large clusters, one major series $(N_2O_3)_yNO^+(pDFB)_z$ and one minor series $[(NO)_3(N_2O_3)_y(pDFB)_z]^+$ can be assigned. As a coincidence, the mass of three N_2O_3 equals that of two *p*DFB molecules (*m/e* = 228). Consequently, for some larger clusters $(N_2O_3)_yNO^+(pDFB)_z$, one peak may correspond to at least two different clusters [e.g. $NO^+(N_2O_3)_3$ and $NO^+(pDFB)_2$]. The mass (M) of cluster peaks in Fig. 2 (top) for the (*p*DFB + NO/Ar) system can be generally fitted to 30 + 38n (n = 2, 3, 4, . . .), and the composition of each cluster peak is listed in Table 1.

The identifications of the composition of the mass peaks in Fig. 2 (top) can be facilitated by examining the intensity distributions of the cluster series and the cluster photodissociation patterns as will be described below. For example, the positive charge appears to be on NO for most NO-containing cluster cations. This is reasonable if one notices that the intensity of $[(NO)_x(N_2O_3)_y(pDFB)_z]^+$ decreases monotonically with y and z but not with x (Fig. 2). Actually, most cluster cations contain only one unit of NO. It is believed that the major contribution to the peaks of larger clusters in the mass spectrum for the (*p*DFB + NO/Ar) system should be the complexes containing *p*DFB molecule(s), instead of $NO^+(N_2O_3)_x$.

Table 1
Composition of the cluster cations, $(N_2O_3)_yNO^+(pDFB)_z$, formed by electron impact ionization, with *m/e* = 30 + (76y + 114z) = 30 + 38n (n = 2, 3, 4, . . .)

m/e	*n*	*y*	*z*
106	2	1	0
144	3	0	1
182	4	2	0
220	5	1	1
258	6	3	0
		0	2
296	7	2	1
334	8	4	0
		1	2
372	9	3	1
		0	3
410	10	5	2
		0	2
448	11	4	1
		1	3
486	12	6	0
		0	4
		3	2
524	13	5	1
		2	3

3.1.2. Photodissociation of $[(NO)_x(N_2O_3)_y(pDFB)_z]^+$ at 456 nm and 700 nm

Shown in Fig. 3 are photodissociation difference mass spectra of two typical cluster cations $NO^+(N_2O_3)$ and $NO^+(pDFB)$ at λ = 456 nm. The difference mass spectra result from the subtraction of a mass spectrum with the dissociation laser "on" from that with the dissociation laser "off." According to Fig. 3, NO^+ is the dominant fragment for

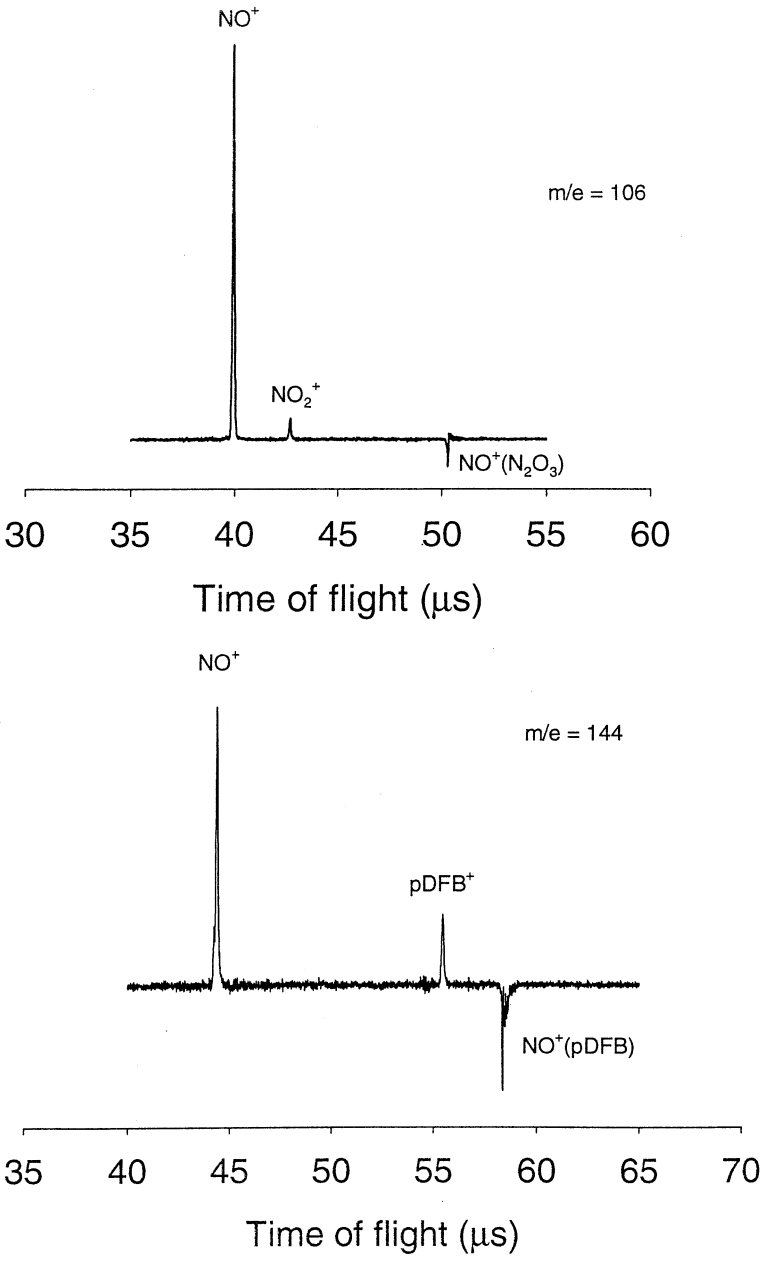

Fig. 3. Difference mass spectra for the photodissociation of $NO^+(N_2O_3)$ and $NO^+(p\text{DFB})$ at $\lambda = 456$ nm. Each mass spectrum was averaged over 100 experimental cycles.

both parents. The composition of the two parents are now ascertained from the photodissociation patterns.

Many other complex cations have been subjected to photodissociation, and their fragmentation patterns are listed in Table 2. It is noticed that many channels are open for the photodissociation of a given cluster cation. Photodissociation of $NO^+(p\text{DFB})$ (m/e = 144) produces both NO^+ and $p\text{DFB}^+$ (Fig. 3), but the former is dominant. Combining the cluster intensity

Table 2
Fragments from photodissociation of $(N_2O_3)_yNO^+(pDFB)_z$ at $\lambda = 456$ nm

m/e	Parent ions	Fragments
106	$NO^+(N_2O_3)$	NO^+, NO_2^+
144	$NO^+(pDFB)$	NO^+, $pDFB^+$
166	$(NO)_3^+(N_2O_3)$	NO^+, NO_2^+, $(NO)_2^+$, $N_2O_3^+$, $NO^+(N_2O_3)$
182	$NO^+(N_2O_3)_2$	NO^+, NO_2^+, $(NO)_2^+$, $N_2O_3^+$, $NO^+(N_2O_3)$
220	$(N_2O_3)NO^+(pDFB)$	NO^+, NO_2^+, $(NO)_2^+$, $N_2O_3^+$, $pDFB^+$, $NO^+(pDFB)$
258	$NO^+(pDFB)_2$ $NO^+(N_2O_3)_3$	NO^+, $(NO)_2^+$, $NO^+(N_2O_3)$, $PDFB^+$, $NO^+(pDFB)$
296	$(N_2O_3)_2NO^+(pDFB)$	NO^+, NO_2^+, $NO^+(N_2O_3)$, $pDFB^+$, $NO^+(pDFB)$
334	$(N_2O_3)NO^+(pDFB)_2$ $NO^+(N_2O_3)_4$	NO^+, $NO^+(N_2O_3)$, $pDFB^+$, $NO^+(pDFB)$
372	$(N_2O_3)_3NO^+(pDFB)$ $NO^+(pDFB)_3$	NO^+, $(NO)_2^+$, $NO^+(N_2O_3)$, $pDFB^+$, $NO^+(pDFB)$
410	$(N_2O_3)_2NO^+(pDFB)_2$ $NO^+(N_2O_3)_5$	NO^+, $(NO)_2^+$, $NO^+(N_2O_3)$, $pDFB^+$, $NO^+(pDFB)$
448	$(N_2O_3)_4NO^+(pDFB)$ $(N_2O_3)NO^+(pDFB)_3$	NO^+, $(NO)_2^+$, $pDFB^+$, $NO^+(pDFB)$, $(N_2O_3)NO^+(pDFB)$
486	$(N_2O_3)_3NO^+(pDFB)_2$ $NO^+(N_2O_3)_6$ $NO^+(pDFB)_4$	NO^+, $(NO)_2^+$, $pDFB^+$, $NO^+(pDFB)$, $(N_2O_3)NO^+(pDFB)$

distribution described above, we therefore believe that NO is perhaps the main bearer of the positive charge in the complex although its ionization energy (IE) is slightly higher than that of *p*DFB (NO: IE = 9.26 eV; *p*DFB: IE = 19.14 eV) [23,24]. A plausible explanation is that aromatic molecules such as *p*DFB are much more polarizable than NO, and therefore $NO^+(pDFB)$ is significantly more stabilized by the ion–dipole interaction than $pDFB^+(NO)$. The opening of the two channels from photodissociation of $NO^+(pDFB)$ may be attributed to the presence of isomers [$NO^+(pDFB)$ and $NO(pDFB)^+$] or photoinduced charge transfer from *p*DFB to NO^+ in the complexes. However, as will be described below, photodissociation at long wavelengths, e.g. 700 nm, yielded only the NO^+ product. We measured the dependence of the photofragment ion intensity on the laser fluence at $\lambda = 503$ nm and $\lambda = 420$ nm. A linear dependence was found for both NO^+ and $pDFB^+$ fragments, indicating a single-photon process.

Table 2 suggests that all the photofragments can be divided into two categories, depending on whether the fragments contain *p*DFB or not: (A) NO^+, NO_2^+, $(NO)_2^+$, $N_2O_3^+$, $NO^+(N_2O_3)$ and (B) $pDFB^+$, $NO^+(pDFB)$, and $(N_2O_3)NO^+(pDFB)$. Overall, category (A) accounts for most of the fragments, whereas category (B) fragments are minor. For larger complexes, e.g. $m/e > 182$, category (B) fragments tend to catch up with the former. This suggests that when cluster size increases, the positive charge is more and more likely to be localized on the aromatic groups.

Fig. 4 shows the difference mass spectra for the photodissociation of the same van der Waals complexes as in Fig. 3 [$NO^+(N_2O_3)$ and $NO^+(pDFB)$] but at $\lambda = 700$ nm (laser fluence = 15 mJ/pulse). The photodissociation patterns can be directly compared with those in Fig. 3. The most notable difference is that whereas small fragment peaks other than NO^+ appeared at 456 nm, NO^+ becomes the only fragment at $\lambda = 700$ nm. The absence of fragments NO_2^+ and $pDFB^+$ at 700 nm implies that these fragments were produced through photoinduced intracluster charge transfer and intracluster reaction at high photon energy (456 nm). The photodissociation patterns of more extensive complexes are listed in Table 3. In general, photofragmentation is quite extensive at 456 nm, but is much suppressed at 700 nm. In particular, at 700 nm, we failed to observe

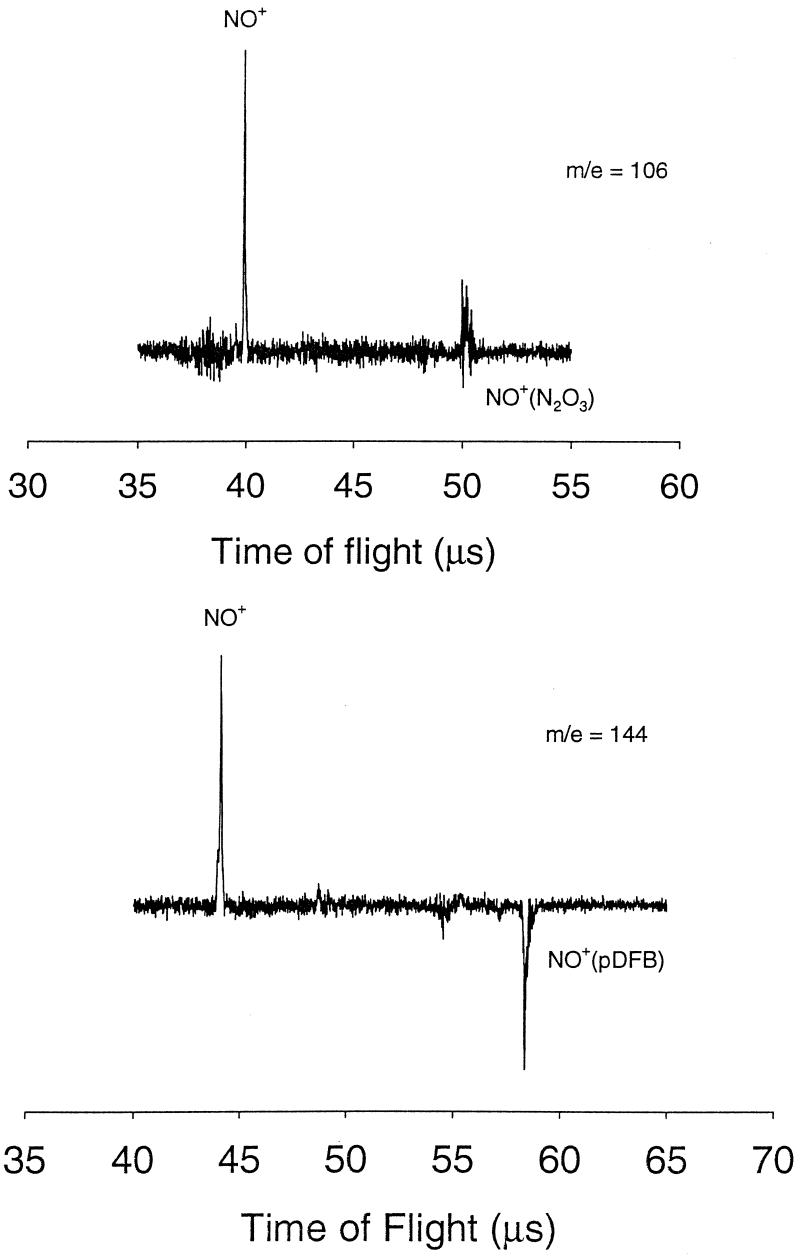

Fig. 4. Difference mass spectra for the photodissociation of $NO^+(N_2O_3)$ and $NO^+(p\text{DFB})$ at $\lambda = 700$ nm (laser fluence = 15 mJ/pulse). Each mass spectrum was averaged over 100 experimental cycles.

any fragment peaks for the parent complex ions $NO^+(N_2O_3)_2$, $(N_2O_3)NO^+(p\text{DFB})$, and $(N_2O_3)_2NO^+(p\text{DFB})$. In addition, the photofragmentation patterns for large parent complexes containing at least two *p*DFB molecules seem to show a decreasing trend in the ion intensities of the category (A) fragments and an increasing trend in the ion intensities of the category (B) fragments.

The above observations may be explained by the assumption that the fragment formation of categories

Table 3
Fragments from photodissociation of $(N_2O_3)_yNO^+(pDFB)_z$ at $\lambda = 700$ nm

m/e	Parent ions	Fragments
106	$NO^+(N_2O_3)$	NO^+
144	$NO^+(p\text{DFB})$	NO^+
182	$NO^+(N_2O_3)_2$	None
220	$(N_2O_3)NO^+(p\text{DFB})$	None
258	$NO^+(p\text{DFB})_2$ $NO^+(N_2O_3)_3$	NO^+, $p\text{DFB}^+$, $NO^+(p\text{DFB})$
296	$(N_2O_3)_2NO^+(p\text{DFB})$	None
334	$(N_2O_3)NO^+(p\text{DFB})_2$ $NO^+(N_2O_3)_4$	$p\text{DFB}^+$, $NO^+(p\text{DFB})$
372	$(N_2O_3)_3NO^+(p\text{DFB})$ $NO^+(p\text{DFB})_3$	$p\text{DFB}^+$, $NO^+(p\text{DFB})$

(A) and (B) proceeds via different excitation processes. The former may be of an electronic origin, in which the excitation energy is far above the dissociation threshold. However, the latter is dominated by a vibrational excitation in the ground state that is thought to be near the dissociation threshold. The exclusive formation of the NO^+ fragment at low photon energy strongly suggests that the positive charge carrier is NO in the cluster cations under study.

3.1.3. Photodissociation spectra of mass-selected dimer cations

Complex ions between mono-fluorobenzene and NO were also produced using the method described above. However, the photodissociation pattern of $NO(FB)^+$ at long wavelengths (~700 nm) appears to be contrary to that of $NO^+(p\text{DFB})$: the main fragment of the former is FB^+, whereas the main fragment of the latter is NO^+. This cannot be explained by ionization energy arguments because the IE of *p*DFB (9.14 eV) is even lower than that of FB (9.20 eV). One would speculate that the two complexes have different geometries, which would then support different electronic structures [$NO(FB)^+$ versus $NO^+(p\text{DFB})$], resulting in different fragmentation channels upon photoexcitation. It would be very interesting to obtain structural information of these complexes by performing high resolution spectroscopy.

We have recorded the photodissociation spectra of $NO(FB)^+$ in a spectral region from 350 nm to 600 nm by monitoring both NO^+ and FB^+, and they are shown in Fig. 5. In general, the fragment intensity increases as the wavelength decreases, and the photodissociation spectra show an envelope peaking at ~380 nm. Around the envelope peak at ~380 nm, the intensity of both fragments NO^+ and FB^+ is of similar amplitude, whereas at long wavelengths (e.g. 600 nm), the fragment FB^+ is predominant. Reproducible sharp peaks with an average spacing of ~1500–1600 cm^{-1} can be identified as shown by the arrows in the figure. This spacing is close to the vibrational progression of the NO species in the complex, which in its free state has $\omega_e = 1904$ cm^{-1} and $\omega_e\chi_e = 14$ cm^{-1} [25]. At short wavelengths, both spectra (obtained by monitoring NO^+ and FB^+) are almost identical. However, the intensity of the NO^+ channel becomes substantially smaller at long wavelengths (>450 nm).

As a comparison, the photodissociation spectrum of $(FB)_2^+$ is shown in Fig. 6. It consists of a small peak at ~420 nm and a much more intense and broader peak at >800 nm. On the basis of previous studies on related systems [26], the small peak at the short wavelength clearly corresponds to the local excitation of the individual FB^+ molecule (through the C $\leftarrow$ X transition of FB^+), whereas the intense peak at the long wavelength is associated with the delocalized excimer excitation. By comparing this spectrum with that of $NO(FB)^+$, the envelope at ~380 nm in the spectrum of $NO(FB)^+$ can be attributed to the local excitation of the individual FB^+ molecule in the complex $NO(FB)^+$. This corroborates our assignment of the electronic structure of $NO(FB)^+$ described above.

3.2. Negative van der Waals cluster complexes $[(NO_2)^-(N_2O_3)_y(pDFB)_z]$

3.2.1. The cluster formation and the photodissociation

Representative negative ion time-of-flight (TOF) mass spectra of the van der Waals clusters are shown in Fig. 7. The cluster anions were formed by the combination of supersonic expansion and electron

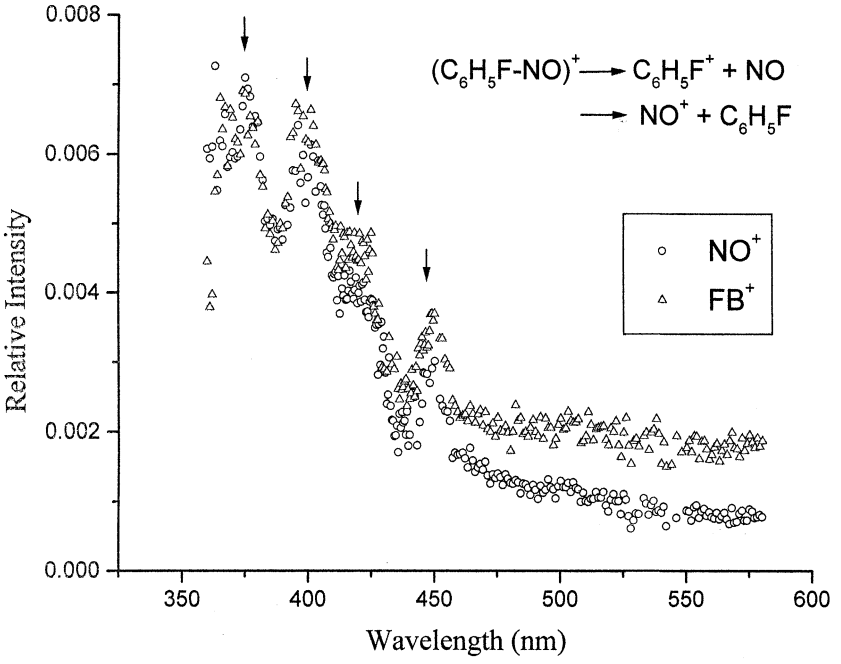

Fig. 5. Photodissociation spectra of $NO(FB)^+$. Both fragments NO^+ and FB^+ were monitored.

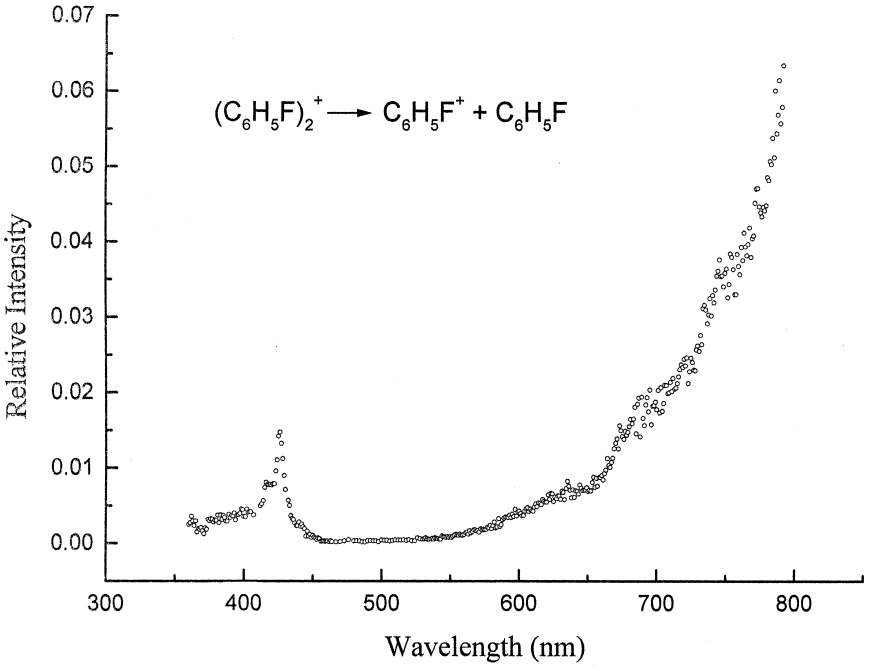

Fig. 6. Photodissociation spectrum of $(FB)_2^+$. The fragment FB^+ was monitored.

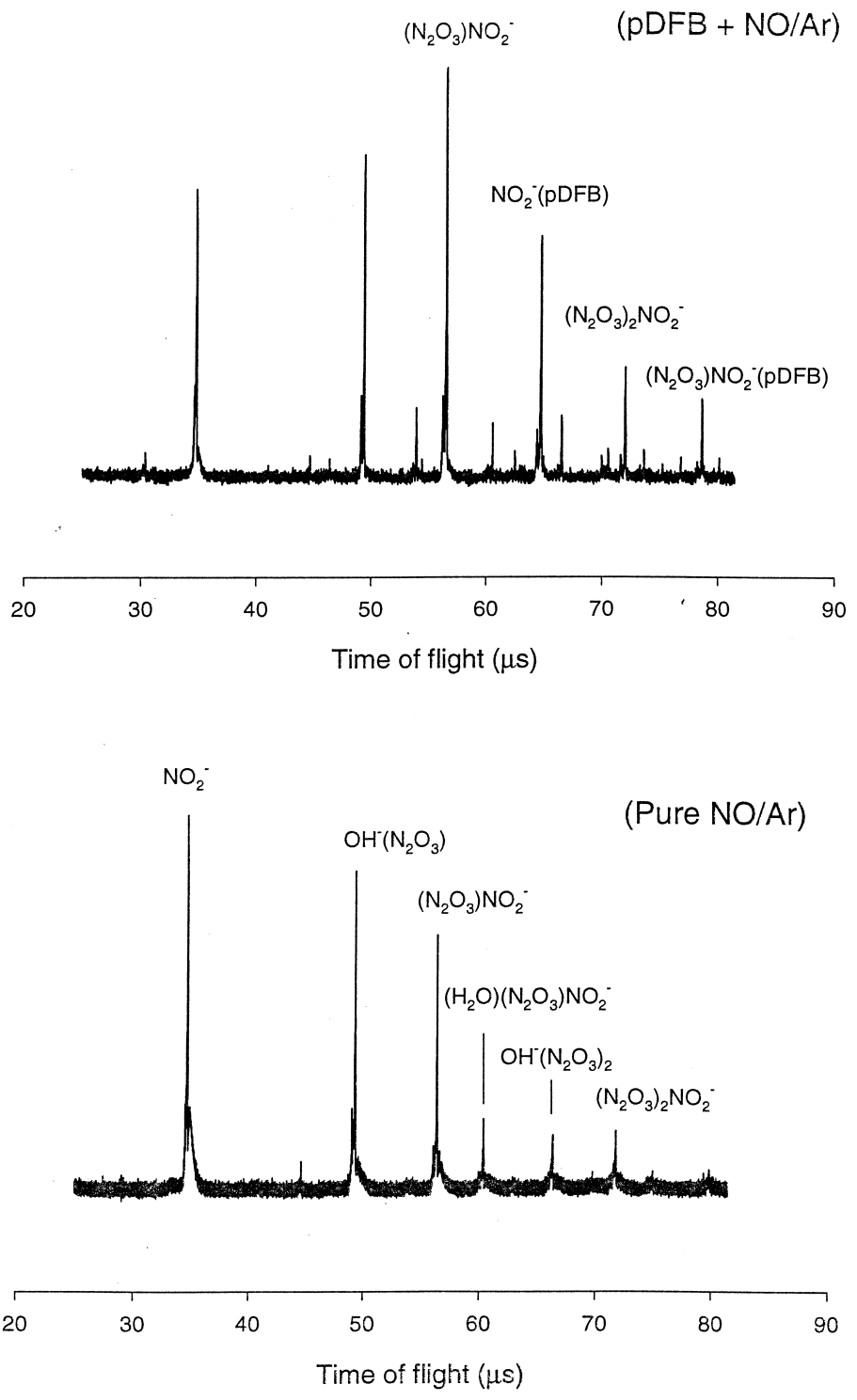

Fig. 7. TOF mass spectra of the van der Waals cluster anions for the system (NO + *p*DFB). Top: with *p*DBF; bottom: without *p*DFB.

impact ionization with *p*DFB present and absent in the mixture, respectively. When no *p*DFB was added, the cluster anions formed were mainly $NO_2^-(N_2O_3)_y$ and $OH^-(N_2O_3)_y$. The existence of N_2O_3 neutral moities in the cluster anions has a similar origin to that in the positive cluster ions. As mentioned above, this type of negatively charged cluster anion, particularly $NO_2^-(N_2O_3)_y$, was reported by Kondow et al. in their Rydberg charge exchange experiments on nitric oxide clusters [21]. When *p*DFB was introduced, the van der Waals complex anions between NO_2 and *p*DFB were formed, and the complexes can be written as $[(NO_2)^-(N_2O_3)_y(pDFB)_z]$. The mass of the cluster series can be expressed by $46 + 38n$ ($n = 2, 3, 4, \ldots$).

Photodissociation of cluster anions was carried out in the same way as in the cation experiments described above. Two difference mass spectra for the photodissociation of NO_2^- (N_2O_3) and $NO_2^-(pDFB)$ at $\lambda = 456$ nm are shown in Fig. 8. NO_2^- is the only charged fragment in both cases due apparently to the high stability of this anion.

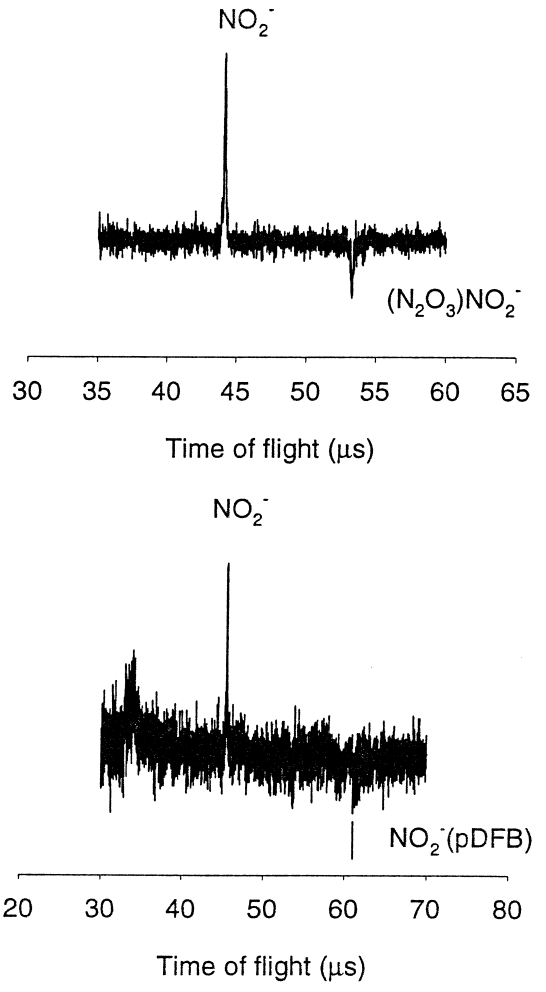

Fig. 8. Difference mass spectra for the photodissociation of $NO_2^-(N_2O_3)$ and $NO_2^-(pDFB)$ at $\lambda = 456$ nm. Each mass spectrum was averaged over 100 experimental cycles.

3.2.2. Photodetachment of $[(NO_2)^-(N_2O_3)_y(pDFB)_z]$

We carried out the photodetachment experiment on the van der Waals complex anions by reversing the polarity of the MCP2 detector after successfully recording the TOF mass spectrum in the linear mode. The parent anions were reflected by the high negative voltage on the detector (MCP2), and only the neutral species resulting from anion photodetachment could arrive at the detector. A difference mass spectrum for the photodetachment experiment is obtained by subtracting a laser-on mass spectrum from a laser-off mass spectrum.

The photodetachment products at $\lambda = 456$ nm are shown in Fig. 9 for NO_2^-, $NO_2^-(N_2O_3)$, and $NO_2^-(N_2O_3)_2$. Because the electron affinity of NO_2 is 2.273 eV [24], which is below the photon energy at 456 nm (2.7 eV), it is understandable that NO_2^- and $NO_2^-(N_2O_3)_{1-2}$ can be photodetached. But it is surprising that no photodetachment product for $NO_2^-(pDFB)$ is observed. This suggests that the extra electron may be delocalized in the whole complex, resulting in a structure with perhaps a higher electron affinity than that of NO_2 (2.273 eV).

4. Summary

Photodissociation/photodetachment of the van der Waals cluster ion system (FB + NO) produced by electron impact ionization has been studied using TOF mass spectrometry. The photodissociation of $(N_2O_3)_yNO^+(pDFB)_z$ has been carried out at $\lambda = 456$ nm and $\lambda = 700$ nm. At 456 nm, photodissocia-

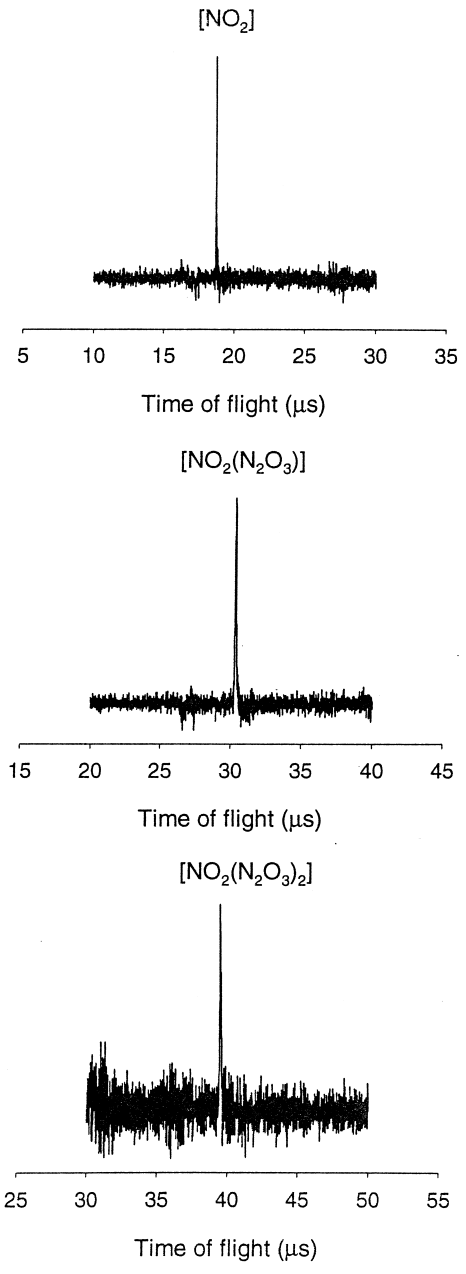

Fig. 9. Difference mass spectra for the photodetachment of $NO_2^-(N_2O_3)_{0-2}$ at $\lambda = 456$ nm. Each mass spectrum was averaged over 100 experimental cycles.

tion is extensive, whereas the photodissociation cross section is substantially smaller at 700 nm and some parent cluster ions cannot be photodissociated. Photodissociation spectra of mass-selected $NO(FB)^+$ and $(FB)_2^+$ were recorded in the UV-visible spectral region. The spectrum of $NO(FB)^+$ revealed excitation of the FB^+ moiety with modulation of the NO vibrational frequency. For $(FB)_2^+$, aside from a localized excitation peak, an excimer band was observed.

Experiments on the complex anion, $NO_2^-(N_2O_3)_y$, revealed competition between photodissociation and photodetachment. But for the complex anion, $NO_2^-(p\text{DFB})$, only a photodissociation channel was observed. This phenomenon is explained by the delocalization of the extra electron, which may result in a higher electron affinity than NO_2 (2.273 eV), and therefore cannot be photodetached by a single photon at 456 nm.

Acknowledgement

This work was supported by an RGC grant administered by the UGC of Hong Kong.

References

[1] E.R. Bernstein, Atomic and Molecular Clusters, Elsevier, Amsterdam, 1990.
[2] R. Schinke, Photodissociation Dynamics, Cambridge University Press, Cambridge, 1993.
[3] (a) K. Ohashi, N. Nishi, J. Chem. Phys. 98 (1993) 390; (b) R. Sussmann, H.J. Neusser, J. Chem. Phys. 102 (1995) 3055; (c) T.L. Grebner, R. Stumpf, H.J. Neusser, Int. J. Mass Spectrom. Ion Processes 167/168 (1997) 649.
[4] (a) Y. Hu, W. Lu, S. Yang, J. Photochem. Photobiol A: Chem. 106 (1997) 91; (b) Y. Hu, W. Lu, S. Yang, Chem. Phys. 218 (1997) 325; (c) W. Lu, Y. Hu, S. Yang, J. Chem. Phys. 108 (1998) 12; (d) W. Lu, S. Yang, J. Phys. Chem. A. 102 (1998) 825.
[5] R.P. Wayne, Chemistry of the Atmospheres, Oxford University Press, Oxford, 1991.
[6] J.S. Stamler, D.J. Singel, J. Loscalzo, Science 258 (1992) 1898.
[7] S.H. Snyder, Science 257 (1992) 494.
[8] H.-J. Galla, Angew. Chem. Int. Ed. Engl. 32 (1993) 378.
[9] H.S. Carman Jr., J. Chem. Phys. 100 (1994) 2629.
[10] D.B. Smith, J.C. Miller, J. Chem. Soc. Faraday Trans. 86 (1990) 2441.
[11] S.R. Desai, C.S. Feigerle, J.C. Miller, J. Chem. Phys. 101 (1994) 4526.
[12] C.A. Woodward, J.F. Winkel, A.B. Jones, A.J. Stace, Chem. Phys. Lett. 206 (1993) 49.

[13] J.F. Winkel, A.B. Jones, C.A. Woodward, D.A. Kirkwood, A.J. Stace, J. Chem. Phys. 101 (1994) 9436.
[14] S. Atrill, A. Mouhandes, J.F. Winkel, A. Goren, A.J. Stace, Faraday Discuss. 102 (1995) 339.
[15] A. Mouhandes, A.J. Stace, Int. J. Mass Spectrom. Ion Processes 159 (1996) 185.
[16] X. Yang, Y.H. Hu, S.H. Yang, J. Chem. Phys. 111 (1999) 7837.
[17] (a) M.E. Nadal, P.D. Kleiber, W.C. Lineberger, J. Chem. Phys. 105 (1996) 504; (b) T. Tsukuda, H. Yasumatsu, T. Sugai, A. Terasaki, T. Nagata, T. Kondow, J. Phys. Chem. 99 (1995) 6367; (c) H. Yasumatsu, A. Terasaki, T. Kondow, J. Chem. Phys. 106 (1997) 3806; (d) D.W. Arnold, S.E. Bradforth, E.H. Kim, D.M. Neumark, J. Chem. Phys. 102 (1995) 3510.
[18] D.S. Cornett, M. Peschke, K. Laihing, P.Y. Cheng, K.F. Willey, M.A. Duncan, Rev. Sci. Instrum. 63 (1992) 2178.
[19] D. Golomb, R.E. Good, J. Chem. Phys. 49 (1968) 4176.
[20] R.G. Orth, H.T. Jonkman, J. Michl, J. Am. Chem. Soc. 103 (1981) 1564; J. Am. Chem. Soc. 104 (1982) 1834.
[21] T. Kondow, in Electronic and Atomic Collisions, D.C. Lorents, W.E. Meyerhof, J.R. Peterson (Eds.), Elsevier Science, Amsterdam, 1986, p. 517.
[22] M.Z. Martin, S.R. Desai, C.S. Feigerle, J.C. Miller, J. Phys. Chem. 100 (1996) 8170.
[23] G.K. Jarvis, M. Evans, C.Y. Ng, K. Mitsuke, J. Chem. Phys. 111 (1999) 3058.
[24] CRC Handbook of Chemistry and Physics, 77th edn., David R. Lide, ed. CRC, Boca Raton, FL, 1996/1997.
[25] K.P. Huber, G. Herzberg, Molecular Spectra and Molecular Structure, IV Constant of Diatomic Molecules, Van Nostrand Reinhold, New York, 1979.
[26] (a) Y. Inokuchi, K. Ohashi, M. Matsumoto, N. Nishi, J. Phys. Chem. 99 (1995) 3416; (b) K. Ohashi, Y. Inokuchi, N. Nishi, Chem. Phys. Lett. 257 (1996) 137; (c) K. Ohashi, Y. Inokuchi, N. Nishi, Chem. Phys. Lett. 263 (1996) 167; (d) Y. Nakai, K. Ohashi, N. Nishi, J. Phys. Chem. A 101 (1997) 472; (e) M. Matsumoto, Y. Inokuchi, K. Ohashi, N. Nishi, J. Phys. Chem. A 101 (1997) 4574; (f) K. Ohashi, Y. Nakane, Y. Inokuchi, Y. Nakai, N. Nishi, Chem. Phys. 239 (1998) 429.